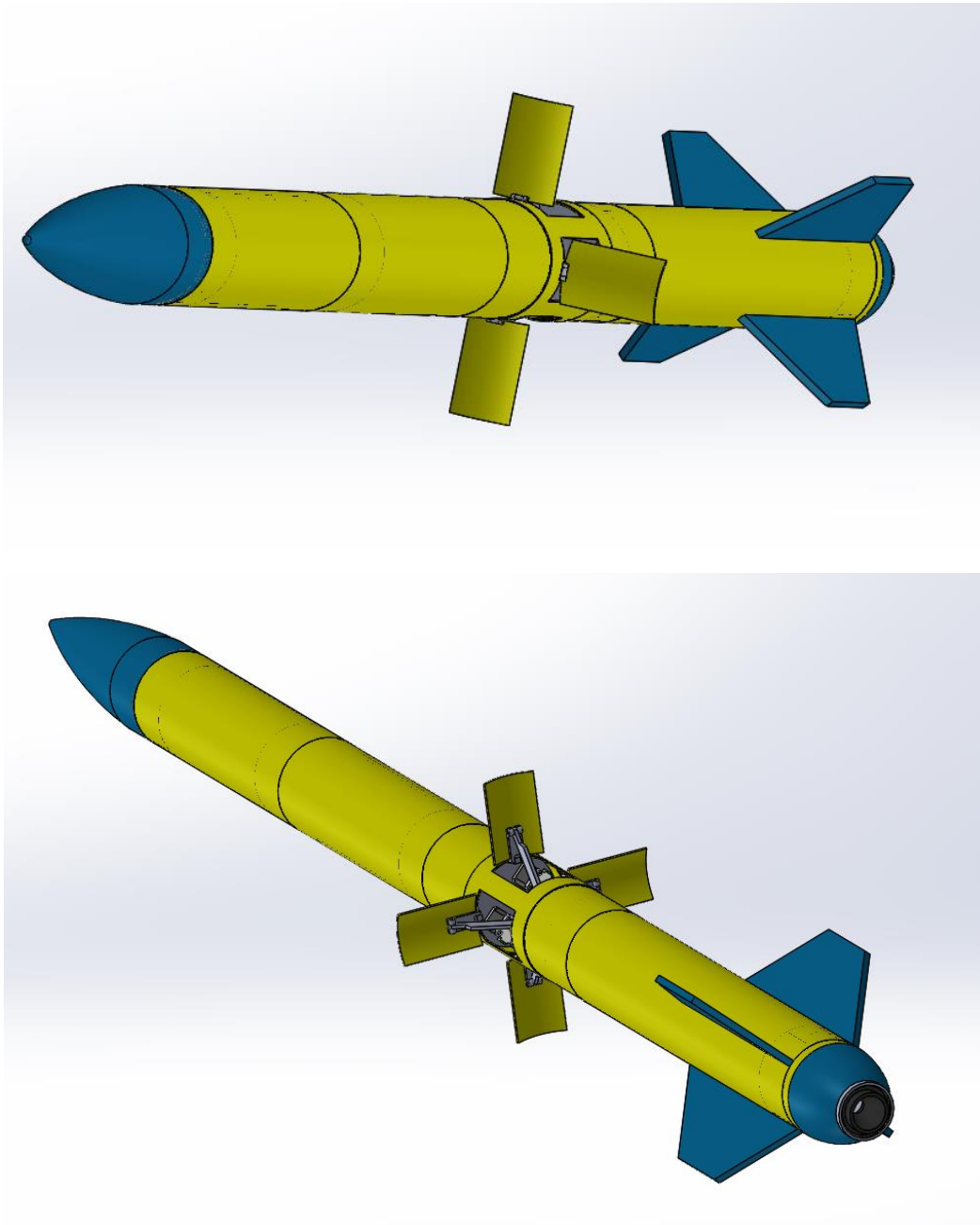


# ***Drag Modulation of a Sounding Rocket***

## **Mechanical Overview**

Robert “Casey” Wilson



### ***Executive Overview:***

To achieve a desired apogee in sounding rocket competitions, a drag modulation or ‘active drag’ system is under development. This report is an overview of the mechanical design and analysis of the system. Some aerodynamic modelling was performed for an estimate of flap force for various deflection angles and velocities. As of now, no power or control system has been developed.

### ***Kinematic Analysis:***

The drag modulation system consists of four, 1 DOF, 4-bar mechanisms that deflect aerodynamics flaps. The mechanisms share a common ground link and actuation link. The actuation link is a lead screw/nut system. From the dimensions of the Solidworks model, the positional representation was created in figure 1. Shown as a comparison is a capture of the 4-bar mechanism.

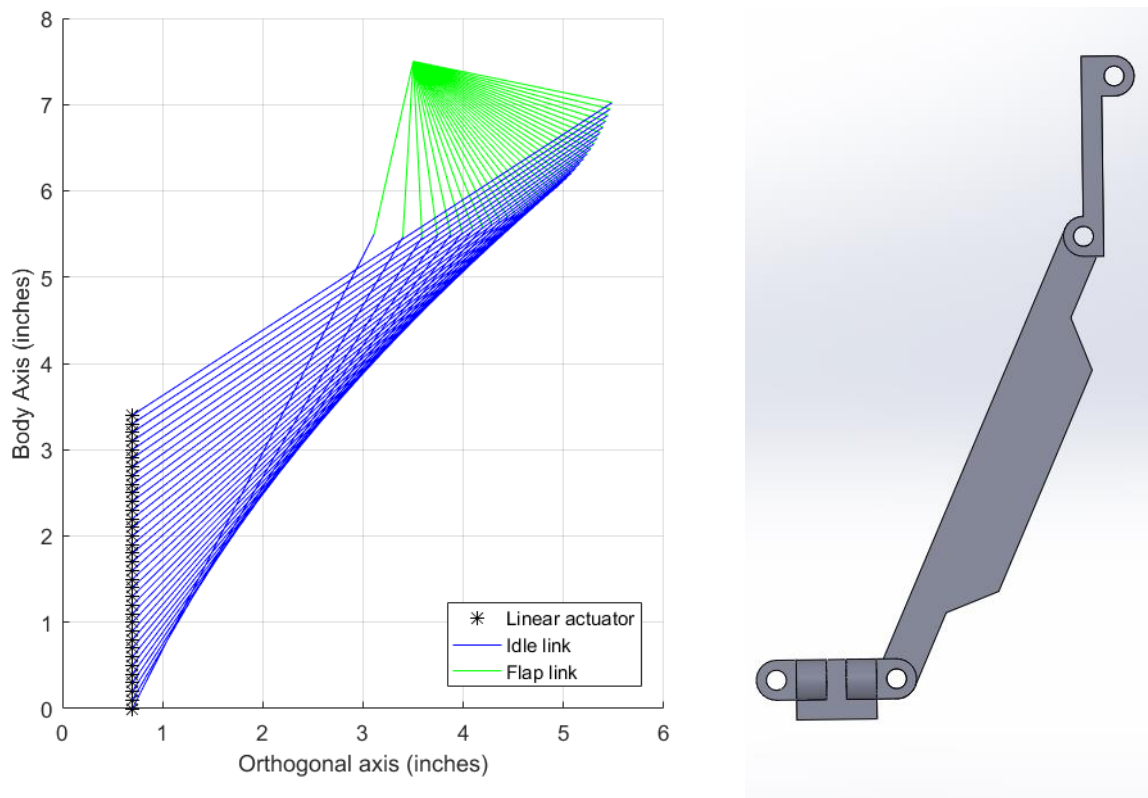


*Figure 1. Positional representation with model comparison.*

To characterize the motion of the mechanism, an analysis was defined to determine the linearity between the actuation of the input link and the angular deflection of the flap link. The subplots in figure 2 shows this relationship and two forms of residual error.

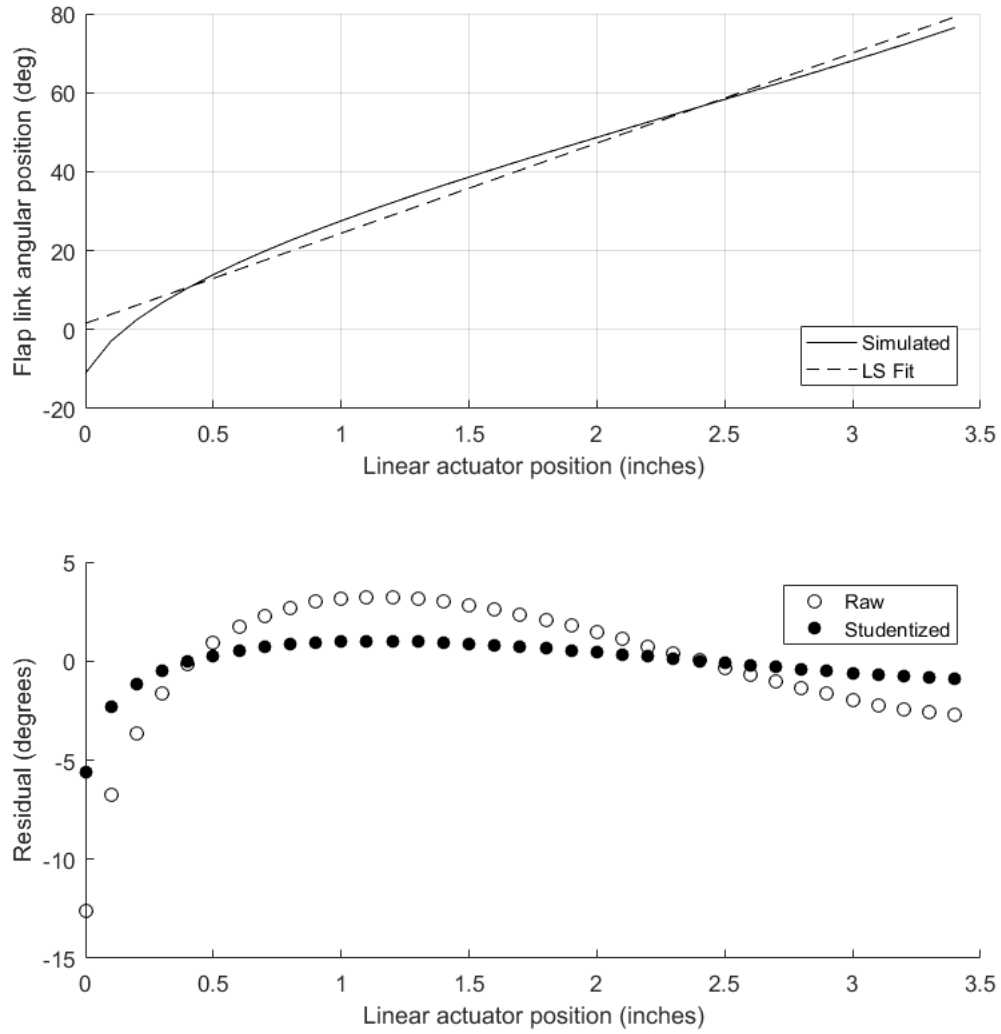


Figure 2. LSF of input link/ flap link kinematic relationship and residual representation.  $R^2 = 0.9803$

From the high  $R^2$  value, some further analyses choose to linearize the relationship in the first subplot.

### ***Force analysis***

The force analysis of the mechanism was defined as a first step to reliable component design. The most prevalent failures would be the buckling of an idle link or the shear failure of a joint pin. To determine the forces that would act on the flaps at a specified angle of attack, an airfoil analysis tool known as XFLR5 was used to determine the drag coefficient on an (effectively) flat plate from 0 to 32 degrees. Beyond 32 degrees the software would not converge to a solution. To estimate a value for  $C_d$  at higher angles of attack than 32 degrees, a linear extrapolation was performed. Wind tunnel or CFD analysis of the entire mechanism will be required for more realistic force modeling and eventual flight prediction. Matrix force analysis was used to determine the pseudo-static forces acting on the links. For brevity and importance, attention will only be paid to the actuation link. Forces on this link will affect the plurality of the low-level actuator and power design.

Figure 3 shows the relationship between the deflection of the flap and the forces on the input link for a 500ft/sec deployment. This is an example to demonstrate the behavior of the resultant force as the angle of attack of the flap increases. For a more conservative estimate, the air density was assumed to be at SSL conditions. A more robust force representation is shown below.

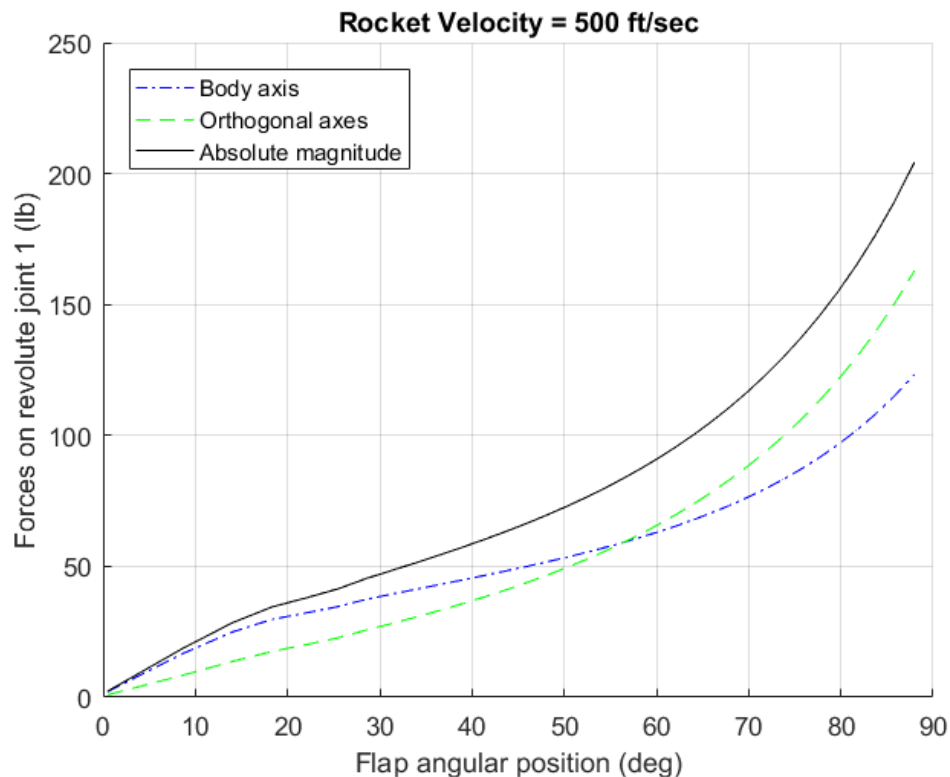


*Figure 3. Forces on input link joint for 500 ft/sec deployment*

To more accurately define a ‘flight envelope’ for the system – that is, at what conditions the system can operate nominally, an analysis of forces on the mechanisms over a range of deflections and rocket velocities was defined. Figure 4 represents the results of this analysis. Note that figure 4 represents the *total* body axis force on the input link. Because of this, the force from all four, 4-bar mechanism actuators are included.

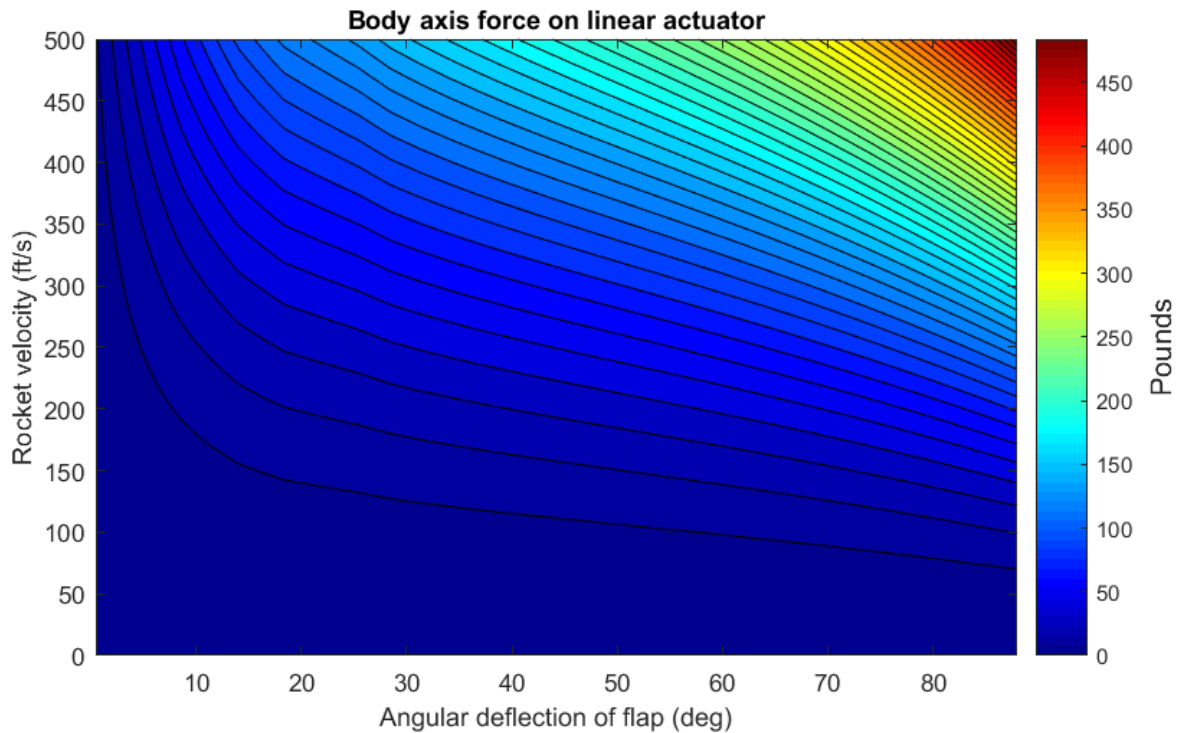
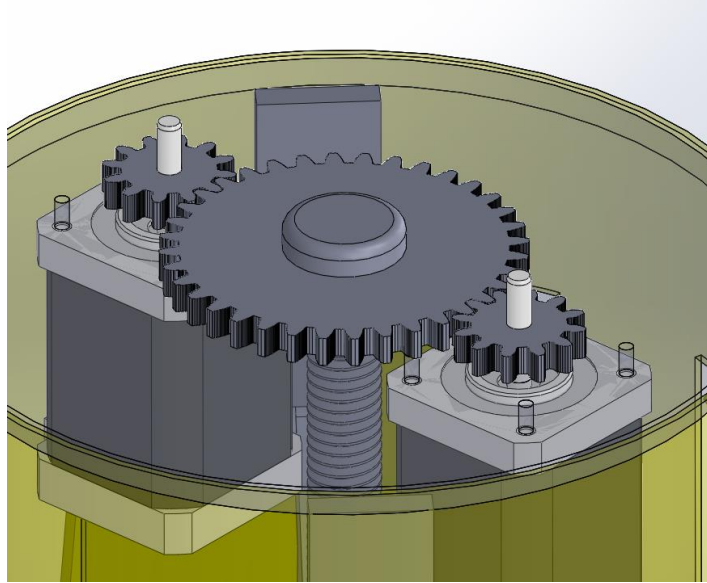


Figure 4. Contour representation of body-axis forces on actuator joint.

### ***Actuator analysis***

To provide actuation for the system, a motor configuration with a large holding torque was required. Initially, stepper motors were suggested. After the preliminary force analysis, a pair of NEMA MS17HDBP4150 motors were chosen to provide actuation. An overall gear ratio of 30:1 is provided by a system of spur gears and an ACME threaded rod with pitch of 10 TPI. The central spur gear that drives the rod is parented by two identical 3:1 ratio gears uniaxial with the stepper bearing. Figure 5 shows this setup in the Solidworks model.



*Figure 5. 30:1 linear drive train. Stepper motors actuate in tandem and provide double torque and reduce cyclic loads on lead screw during operation. Center of mass of the system is also conserved in this configuration.*

From the manufacturer's specifications, the following angular velocity – torque relationship was constructed. Figure 6 was provided by the manufacturer.

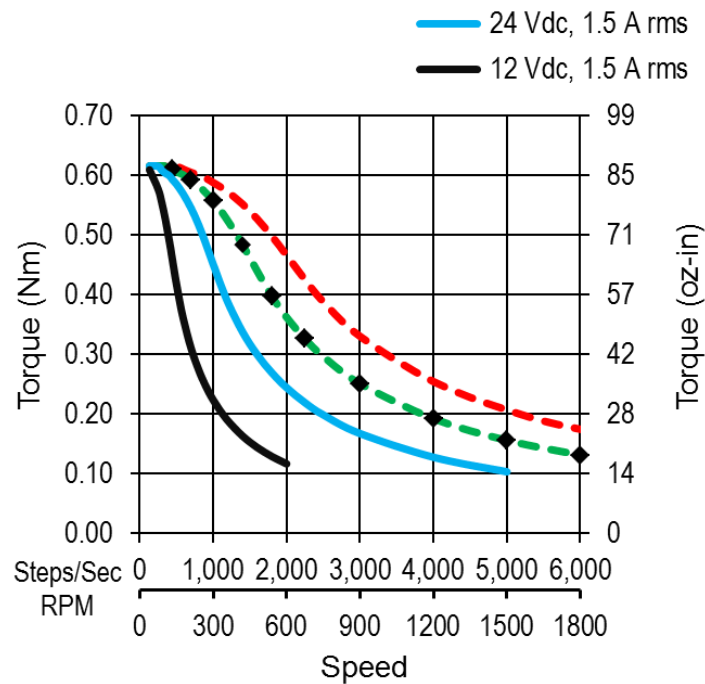


*Figure 6. Torque-speed curve*

From the gear ratio and speed curve above, it was possible to determine the maximum positive flap angular velocity for a set of flight speeds and actuator positions. If the zero-speed actuation force was less than the static aerodynamically induced force on the input link, the maximum speed was assumed to be 0 degrees/second. Likewise, for many angular deflection / rocket velocity combinations, the speed of the actuation could be approximated as its no-load speed. Figure 7 and 8 show these relationships for the 12V and 24V, 1.5 A power supply curves. These power options were deemed most practical for the system.

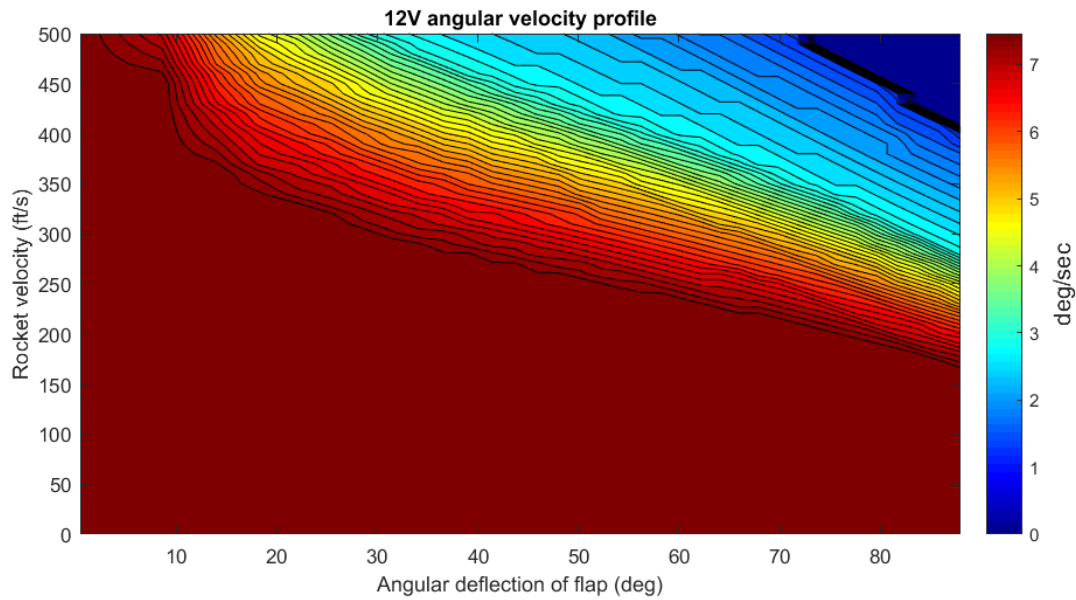


*Figure 7. Flap speed profile for 12V source*

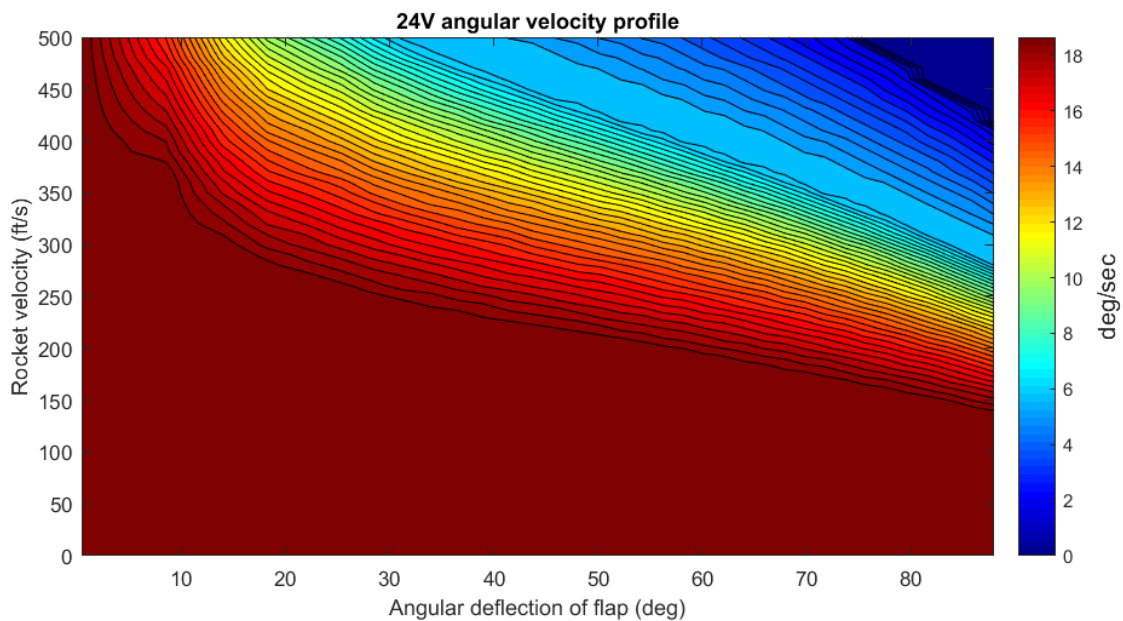


*Figure 8. Flap speed profile for 24V source*

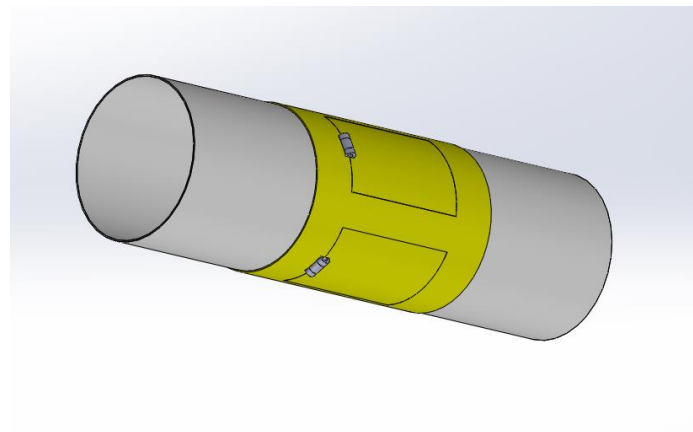
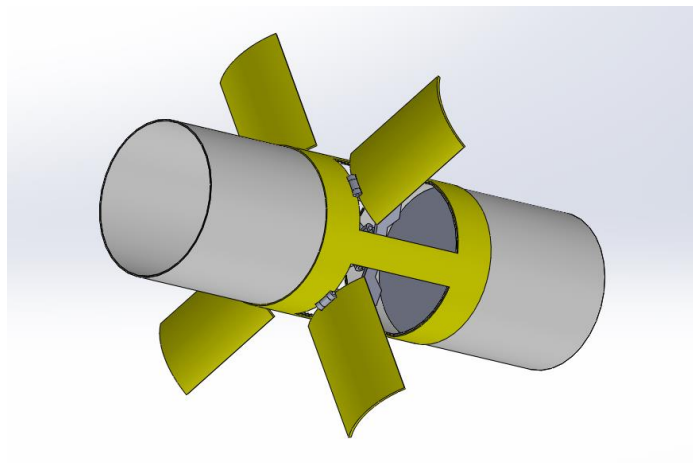
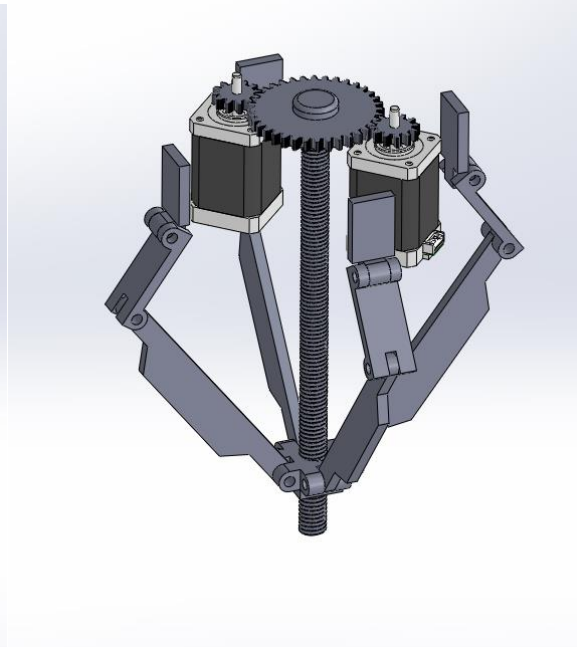
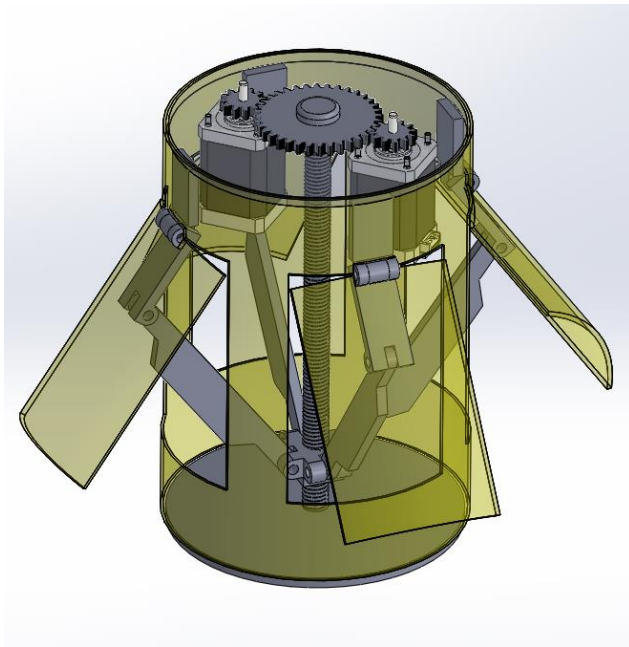
### ***Conclusion and future works***

The mechanical analysis and design outlined in this paper will serve as a ground on which to further design the system. Of the 3-pronged holistic system phalanx, the aerodynamic and control/electronic subsystems are largely undeveloped.

A further step in the mechanical design will be to analyze the components at their maximum performance stresses using both manual calculation and an FEA software such as ANSYS. A redesign of either the gear ratio or an alternation in steppers motors may be made to facilitate faster flap deflection for the 12V option.



APPENDIX A. Isometric CAD views of the mechanism and modular system



## APPENDIX B. ½ scale prototype

